SCISPACE
formerly Typeset

Open access • Journal Article • DOI:10.1063/5.0003628

The role of iron in magnetic damping of Mg(Al,Fe)2O4 spinel ferrite thin films

— Source link

Jacob J. Wisser, Jacob J. Wisser, Lauren Riddiford, Lauren Riddiford ...+9 more authors

Institutions: Geballe Laboratory for Advanced Materials, Stanford University, Auburn University, Virginia Tech ...+2 more institutions

Published on: 10 Apr 2020 - Applied Physics Letters (AIP Publishing LLC AIP Publishing)

Topics: Magnetic damping, Magnetization, Ferromagnetic resonance, Magnetic moment and Magnetic circular dichroism

Related papers:

- Magnetic Properties of Co-doped Fe2O3 Thin Films
- Structural, electrical, and magnetic properties of Mn2.52–xCoxNi0.48O4 films
- MAGNETIC PROPERTIES OF GRANULAR Fe-Cu AND Fe-Ag ALLOYS
- Magnetic properties of the Co–C60 and Fe–C60 nanocrystalline magnetic thin films
- Magnetic and structural properties of Mn-Ga thin films

Share this paper:

View more about this paper here: https://typeset.io/papers/the-role-of-iron-in-magnetic-damping-of-mg-al-fe-2o4-spinel-3tooo46lw3

Lawrence Berkeley National Laboratory
Recent Work

Title
The role of iron in magnetic damping of Mg(Al,Fe)2O4 spinel ferrite thin films

Permalink
https://escholarship.org/uc/item/9j55r5wx

Journal
Applied Physics Letters, 116(14)

ISSN
0003-6951

Authors
Wisser, JJ
Riddiford, LJ
Altman, A
et al.

Publication Date
2020-04-06

DOI
10.1063/5.0003628

Peer reviewed

eScholarship.org Powered by the California Digital Library
University of California

The role of iron in magnetic damping of $Mg(Al,Fe)_2O_4$ spinel ferrite thin films

Jacob J. Wisser,[1,2] Lauren J. Riddiford,[1,2] Aaron Altman,[3] Peng Li,[4] Satoru Emori,[5] Padraic Shafer,[6] Christoph Klewe,[6] Alpha T. N'Diaye,[6] Elke Arenholz,[7] and Yuri Suzuki[1,2]

[1]*Department of Applied Physics, Stanford University, Stanford, California 94305, USA*
[2]*Geballe Laboratory for Advanced Materials, Stanford University, Stanford, California 94305, USA*
[3]*Department of Applied Physics, Stanford University, Stanford, CA , USA*
[4]*Department of Electrical and Computer Engineering, Auburn University, Auburn, Alabama 36849, USA*
[5]*Department of Physics, Virginia Tech, Blacksburg, Virginia 24061, USA*
[6]*Advanced Light Source, Lawrence Berkeley National Laboratory, Berkeley, California 94720, United States*
[7]*Cornell High Energy Synchrotron Source, Cornell University, Ithaca, New York 14853, United States*

We have investigated magnesium aluminum ferrite thin films with a range of iron concentrations and identified the optimal iron content to obtain high crystalline quality thin films with the low magnetic damping required for spin current–based applications. Epitaxial $MgAl_{2-x}Fe_xO_4$ films with 0.8<x< 2.0 were grown by pulsed laser deposition (PLD) on single crystal $MgAl_2O_4$ (MAO) substrates and were characterized structurally and magnetically. We find that the $x = 1.5$ composition minimizes the room-temperature magnetic damping with a typical Gilbert damping parameter of $\alpha_{eff} = 1.8 \times 10^{-3}$. This minimized damping is governed by a competition between the more robust magnetic ordering with increased iron content, x, and the more defective structure due to larger film–substrate lattice mismatch with increased iron content. The temperature-dependent magnetization curves indicate that T_c is suppressed below room temperature for iron content $x \leq 1.2$ and eventually suppressed entirely for $x = 0.8$. X-ray magnetic circular dichroism results indicate that for all x the magnetic moment is dominated by Fe^{3+} cations distributed in a 60:40 ratio on the octahedral and tetrahedral sites, with minimal contribution from Fe^{2+} cations. Films with $x = 1.4 - 1.6$ exhibit very strong ferromagnetic resonance and low Gilbert damping with $\alpha_{eff} = (1.8 - 6) \times 10^{-3}$, making them ideal candidates for microwave and spintronic applications.

Spinel ferrites have long been studied as more cost-effective alternatives to garnet ferrites for high-frequency microwave applications.[1–4] Of particular importance for pure spin current generation and above resonance circulators are materials with a narrow ferromagnetic resonance (FMR) linewidth and low Gilbert damping. [1, 5, 6] Garnet ferrites have been incorporated in heterostructures demonstrating spin current generation and spin current switching. [7–13] In addition, doping studies on $Y_3Fe_5O_{12}$ (YIG) and barium ferrite with various metallic cations have allowed for modulation of the structural and magnetic properties. These studies have shown favorable results for decreasing the resonance linewidth. [14–17] As an alternative to the garnet ferrites, we have recently reported doped nickel and magnesium ferrites with resonance linewidths as low as ≈5 Oe at 10 GHz and Gilbert damping parameters as low as α <0.002.[18–22] These previous studies have demonstrated both the viability of spinel ferrites as low-loss spin current sources and the versatility of the spinel crystal structure. We have also recently reported that the spinel ferrite $MgAl_{0.5}Fe_{1.5}O_4$ (MAFO) has a number of advantages over YIG, including lower external field requirements for magnetization precession and lower growth temperatures (450 °C as opposed to ≈750 °C for the garnet ferrites). Most recently, we have demonstrated successful spin pumping from spinel ferrites into heavy metals and isostructural integration with other spinel ferrites. [20, 22, 23]

To date, $MgAl_{0.5}Fe_{1.5}O_4$ is the most promising low-loss magnetic insulator among epitaxial spinel ferrite thin films.[19–21] This particular composition of MAFO exhibits a Gilbert damping parameter as low as $\alpha \approx 0.0015$. In order to understand the role of iron stoichiometry on damping in magnesium aluminum ferrite films, we have studied the structure, composition, static magnetic, and ferromagnetic resonance properties of a series of $MgAl_{2-x}Fe_xO_4$ films where $x = 0.8 - 2.0$. As the composition varies from $x = 0.8$ to 2.0, the lattice mismatch with the $MgAl_2O_4$ substrate increases. Although all films exhibit epitaxy and are coherently strained to the substrate as evident from reciprocal space mapping, films with $x = 1.8$ and 2.0 show evidence of decreased film quality and increased mosaic spread. Temperature-dependent magnetization measurements show that films with $x \leq 1.2$ undergo magnetic transitions below room temperature with ferrimagnetic order completely suppressed for $x = 0.8$ in the measured temperature range. Room-temperature magnetic hysteresis loops show that films with $1.4 \leq x \leq 1.6$ exhibit coercivities $H_c < 0.5$ mT, with $x \geq 1.8$ films showing increased coercivities corresponding to the decreased film quality seen in XRD. X-ray magnetic circular dichroism (XMCD) indicated that in all compositions, the magnetism is dominated by Fe^{3+} cations. Finally, Gilbert damping parameters extracted from room temperature ferromagnetic resonance measurements range from $\alpha_{eff} = (1.8 - 6) \times 10^{-3}$ with the $x = 1.5$ composition yielding the lowest damping parameter. From these results we can conclude that $MgAl_{0.5}Fe_{1.5}O_4$ represents a compromise between a large

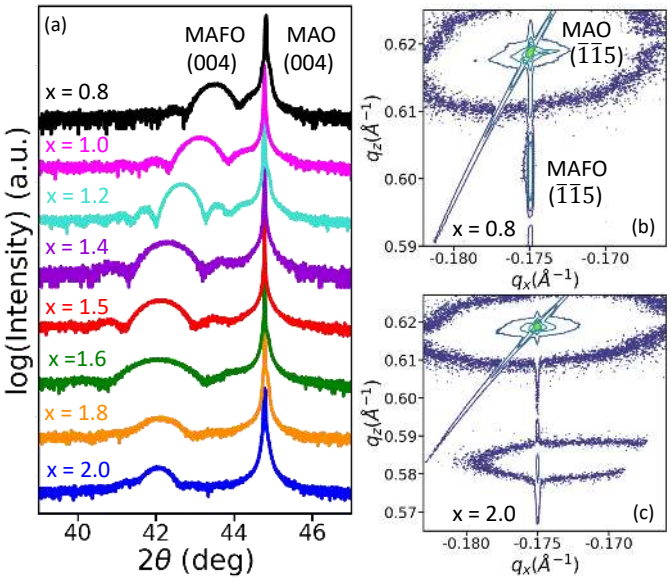

FIG. 1. (a) $2\theta - \omega$ XRD scans for 11 nm thick films with different iron contents showing clear Laue oscillations for $x \leq 1.6$. There is also a systematic increase in the out-of-plane lattice parameter as the iron content is increased up to $x = 1.6$. Labels correspond to the iron content. (b) RSM of the $(\bar{1}\bar{1}5)$ Bragg reflection of an $x = 0.8$ film showing that the film is coherently strained to the substrate. (c) RSM of the $(\bar{1}\bar{1}5)$ Bragg reflection of an $x = 2.0$ film, which is also coherently strained.

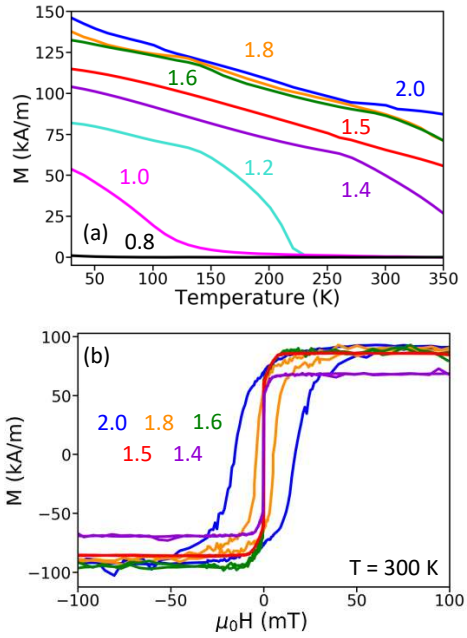

FIG. 2. (a) Magnetization measured as a function of temperature. Films with $x = 1.2, 1.0$ undergo ferrimagnetic transitions with $T_C = 225$ and 150 K, respectively. Compositions where $x \leq 0.8$ do not become magnetic in the measured temperature range. (b) Room-temperature magnetic hysteresis loops for the compositions that are magnetic at room temperature.

magnetic moment and a low concentration of lattice defects to yield low damping for application in low-loss spin current generation and microwave device applications.

Epitaxial thin films of MAFO were deposited on as-received (001)-oriented single crystal $MgAl_2O_4$ (MAO) substrates by pulsed laser deposition. A KrF 248nm excimer laser was incident on a pressed stoichiometric target of $MgAl_{2-x}Fe_xO_4$ for $x = 0.8, 1.0, 1.2, 1.4, 1.5, 1.6, 1.8$ and 2.0 with a fluence of $\approx$2 J/cm^2. The depositions were performed at a substrate temperature of 450°C in 10 mTorr of O_2. Deposition rates were calibrated via x-ray reflectivity. All films are approximately 11 nm thick as this was found to be the optimal thickness for the lowest Gilbert damping in $x = 1.5$ films. [19, 21]

In order to structurally characterize our films, we performed x-ray diffraction using a PANanalytical X'Pert reflectometer. Our results show that MAFO films are epitaxial with the underlying MAO substrates and are of high crystalline quality.

Figure 1(a) shows x-ray diffraction scans of MAFO films with varying compositions. Laue oscillations are observed around the (004) Bragg reflection for films with $x < 1.6$, indicating excellent crystallinity. As the iron content is increased, there is a monotonic increase (up to $x = 1.6$) and then saturation in the out-of-plane lattice constant as the films undergo a larger tetragonal distortion to remain coherently strained to the MAO substrate. Figure 1(b) shows a reciprocal space map (RSM) of an $x = 0.8$ film. The alignment of the film and substrate peaks of the $(\bar{1}\bar{1}5)$ Bragg reflection in Figure 1(b) confirms that the film is coherently strained on the substrate. Typical ω-rocking curves for films in the $x \leq 1.6$ range have a full-width at half-maximum of $\approx$0.045-0.060°, which is comparable to the substrate, indicating low mosaic spread and high film crystallinity.

Structural quality of the films deteriorates as x increases to 2.0 ($MgFe_2O_4$) and the lattice mismatch with the underlying substrate increases. For $x = 1.8$ and $x = 2.0$, the Laue oscillations disappear as the film quality degrades. Figure 1(c) shows an RSM of the $(\bar{1}\bar{1}5)$ Bragg reflection of an $x = 2.0$ film. While the film remains coherently strained, the broader peak and the surrounding "cloud" indicates there is a higher degree of film mosaicity than in the lower compositions. This is confirmed by the broader omega rocking curve with a typical full-width at half-maximum of $\approx 0.085°$ for the $x = 1.8, 2.0$ films in contrast to the films with lower iron content.

To characterize the static magnetic properties of our films, the temperature and field dependence of the magnetization was measured using a Quantum Design Evercool SQUID in the reciprocal sample option mode with a sensitivity of 5×10^{-12} Am^2. These measurements indicate that increased iron content is correlated with the Curie temperature as well as the saturation magnetiza-

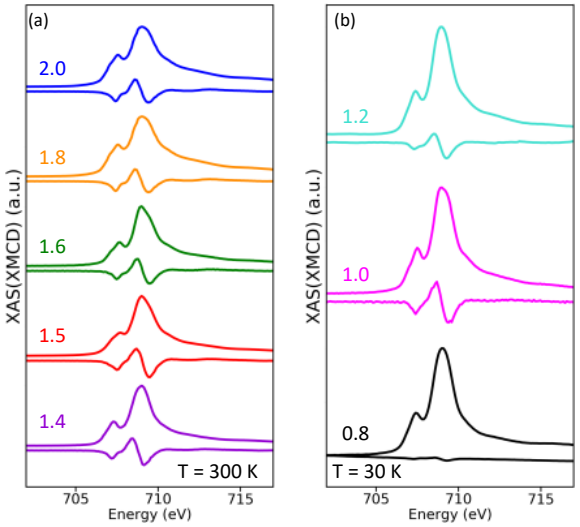

FIG. 3. (a) XAS and XMCD taken at room temperature. (b) XAS and XMCD taken at $T = 30$ K, below the T_C for $x = 1.2$ and 1.0.

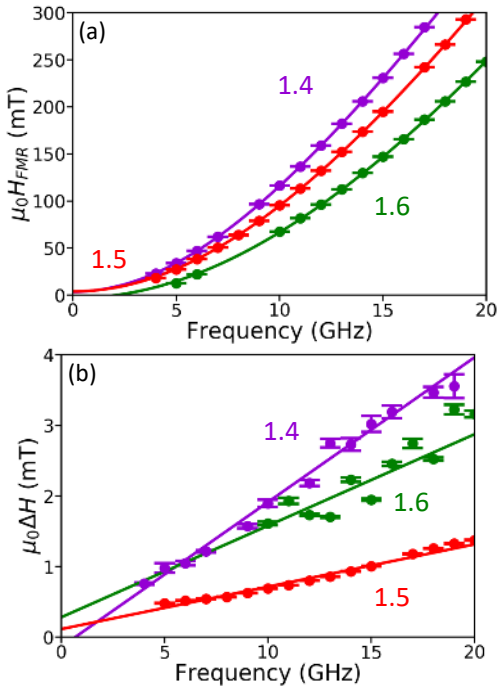

FIG. 4. (a) FMR resonant field as a function of frequency with Kittel equation fits (b) FMR linewidth as a function of frequency with fits to the linewidth equation.

tion.

Magnetization as a function of temperature is shown in Figure 2(a) Films with $1.4 < x < 2.0$ are ferrimagnetic at room temperature, and films with lower iron content of $x = 1.2$ and 1.0 undergo magnetic transitions with $T_C = 225$ and 125K, respectively. There was no detectable magnetic signal in $x = 0.8$ films above the diamagnetic signal of the substrate.

A comparison of the magnetization values at low temperatures for the entire range of iron concentrations indicates that increased iron content increases the overall magnetization of the magnesium aluminum ferrite film. A similar trend is observed at room temperature for those samples that exhibit long range magnetic order as observed in the hysteresis loops taken along the [100] axis for $1.4 \leq x \leq 2.0$ films in Figure 2(b). Films with $1.4 \leq x \leq 1.6$ exhibit very low coercivity ($\mu_0 H_c < 0.5$ mT) and an increasing saturation magnetization with increasing iron content. Films with $x = 1.8$ and 2.0 show much higher coercivities ($\mu_0 H_c = 10$ and 20 mT, respectively) and are slower to saturate. This is likely due to defect pinning and frustrated magnetism attributed to poorer film quality and demonstrates the importance of coherent film growth in obtaining soft magnetism. [24, 25] The static magnetometry results indicate that there is an optimal window of the iron content in the $x = 1.4 - 1.6$ range where the films are ferrimagnetic at room temperature and exhibit soft magnetism that is ideal for spintronic applications such as pure spin current generation and spin-transfer torque.

In order to understand the origin of the soft magnetism in our samples with respect to iron valence and site distribution, we performed x-ray absorption spectroscopy (XAS) and x-ray magnetic circular dichroism (XMCD) at beamlines 6.3.1 and 4.0.2 at the Advanced Light Source at Lawrence Berkeley National Laboratory.

Measurements were performed in an applied field of 400 mT along the circularly polarized x-ray beam, incident at 30° grazing from the film plane. The spectra in Figure 3(a) were taken at room temperature for $1.4 < x < 2.0$, and at $T = 30$ K (below the T_C for $x = 1.2$ and $x = 1.0$) for $0.8 \leq x \leq 1.2$ in Figure 3(b).

The XAS and XMCD (defined as the difference between the + and − polarizations) spectra indicate that the magnetism in our films is derived from Fe^{3+} magnetic ions. In Figure 3, the peak at 709.2 eV is attributed to tetrahedrally coordinated Fe^{3+} and the peak at 710.0 eV to octahedrally coordinated Fe^{3+}[26, 27]. From the XMCD spectra, we note that the octahedrally coordinated Fe^{3+} ions align parallel to the field, while the tetrahedrally coordinated ions align antiparallel to the field. We have also compared our spectra to calculated spectra for Fe^{2+} and do not find that the inclusion of Fe^{2+} improves the fit to our measured XMCD spectra.[28] We note that measurements were performed in the total electron yield configuration, which is only sensitive to the top 5 nm of the sample. It is therefore possible that the bulk of the sample could contain a higher proportion of Fe^{2+} cations, however our ferromagnetic resonance measurements (see below) suggest that this is not the case. The predominance of Fe^{3+} and the absence of any signature of Fe^{2+} is particularly relevant for efficient spin current generation, because Fe^{3+} is an $L = 0$ ion that minimizes magnetic anisotropy and spin-orbit coupling. Experimental reference spectra can be used to determine the distribution of Fe^{3+} ions on the tetrahe-

TABLE I. Summary of Kittel equation and Gilbert damping parameters for the measured compositions.

x	g	$\mu_0 M_{eff}$ (T)	$\lvert H_{4,\parallel}\rvert$ (mT)	$\alpha_{eff}(\times 10^{-3})$
1.4	2.12 ± 0.01	0.90 ± 0.02	9.11 ± 0.17	6.1 ± 0.2
1.5	2.08 ± 0.03	1.19 ± 0.04	8.44 ± 0.10	1.8 ± 0.01
1.6	2.12 ± 0.01	1.55 ± 0.03	8.43 ± 0.11	3.8 ± 0.8

dral (Fe^{3+}_{Th}) and octahedral (Fe^{3+}_{Oh}) sites. We can reproduce our spectra using a combination of $GaFeO_3$ (100% Fe^{3+}_{Oh}) and γ-Fe_2O_3 (37.5% Fe^{3+}_{Th}, 62.5% Fe^{3+}_{Oh}) to give a 60:40 Fe^{3+}_{Oh}:Fe^{3+}_{Th} ratio, as confirmed by our previous study. [19, 26, 27]

Previous dynamic magnetic characterization indicates that we can achieve low magnetic damping with a Gilbert damping parameter as low as <0.002. [19–22] To characterize spin current generation efficiency, we perform broadband FMR measurements at room temperature in a coplanar waveguide setup. The resulting spectra were fit to the sum of the symmetric and antisymmetric components of the Lorentzian derivative, and the resonant field, H_{FMR}, and linewidth, ΔH, were extracted from the fit.

We find that, of the room-temperature ferrimagnets, only the $x = 1.4, 1.5$ and 1.6 compositions show strong FMR (high signal-to-noise ratio) in our setup. Figure 4(a) shows the resonant field, H_{FMR}, as a function of frequency, f, for these compositions. In order to understand this trend, we analyze the frequency dependence of the FMR field in terms of the Kittel equation: [6]

$$f = \frac{g\mu_B}{h}\mu_0 \left[\left(H_{FMR} + H_{4,\parallel}\right)\left(H_{FMR} + M_{eff} + H_{4,\parallel}\right)\right]^{1/2} \quad (1)$$

where g is the Landé g-factor, μ_0 is the permeability of free space, μ_B is the Bohr magneton, h is Planck's constant, $H_{4,\parallel}$ is the in-plane cubic anisotropy field, and M_{eff} is the effective magnetization that accounts for the out-of-plane uniaxial anisotropy field. The three Kittel equation parameters are summarized in Table 1. That $g \approx 2$ for all compositions implies low spin-orbit coupling, as to be expected from the magnetic contribution of Fe^{3+} ions discussed above. In addition, the effective magnetization, M_{eff}, increases as a function of increasing iron content since the saturation magnetization also increases in this composition range. $H_{4,\parallel}$ is approximately 8-9 mT for all measured compositions within experimental error, which is not so surprising given that the strain state (see Figure 1) of the films in this composition range does not vary significantly.

The figure of merit for magnetic damping is the Gilbert damping parameter which is minimized for the $x = 1.5$ iron composition at <0.002. The magnetic damping is deduced from the frequency dependence of the FMR linewidth for $x = 1.4, 1.5$, and 1.6 as shown in Figure 4(b). Fitting the FMR linewidth ΔH as a function of frequency, f, to the linewidth equation yields the Gilbert damping parameter, α_{eff}:

$$\Delta H = \Delta H_0 + \frac{h\alpha_{eff}}{g\mu_0\mu_B} f \quad (2)$$

where ΔH_0 is the zero-frequency linewidth. The Landé g factor is determined via the frequency dependence of the resonant field, as discussed above. From Table 1, we note that the $x = 1.5$ film composition minimizes the Gilbert damping parameter with $\alpha_{eff} = (1.8 \pm 0.01) \times 10^{-3}$, and thus is the best candidate for microwave device low-loss pure spin current generation applications.

According to our FMR results, the $x = 1.5$ composition of MAFO yields the lowest damping parameter. This can be understood from our structural characterization measurements, which indicate the film quality increases as the iron content decreases and the MAFO lattice parameter more closely matches that of the MAO substrate. As the iron content is increased, films undergo more tetragonal distortion to remain coherently strained to the substrate, resulting in a larger mosaic spread for films with $x > 1.6$. Additionally, static magnetization at room temperature suggests that the softest magnetism is observed for $1.4 \leq x \leq 1.6$, which is critical for observing strong FMR signals. Therefore the $x = 1.5$ composition represents an excellent compromise between high enough iron content for magnetic ordering well above room temperature and a low-enough lattice mismatch with the substrate to yield a high quality film with a low concentration of defects. Our results highlight the interplay between film quality, magnetic ordering, and cation chemistry in obtaining films with low magnetic damping.

In summary, we have performed a systematic study of the role of iron content on the structural and magnetic properties of epitaxial $MgAl_{2-x}Fe_xO_4$ films. As the iron content is increased we see a monotonic increase in the out-of-plane lattice parameter and mosaic spread. From static magnetometry, we measure an increase in the Curie temperature as well as the saturation magnetization at low temperatures as the iron content is increased. XAS and XMCD show that the magnetism is derived from Fe^{3+} magnetic moments with minimal spin-orbit coupling. Finally, ferromagnetic resonance studies indicate that the $x = 1.5$ composition gives the lowest Gilbert damping parameter due to a compromise between structural quality and magnetic response. Our results indicate that the $Mg(Al,Fe)_2O_4$ system is an excellent candidate for pure spin current sources, and demonstrates the versatility of the spinel crystal structure for obtaining a wide range of structural and magnetic properites.

This work was supported by the U.S. Department of

Energy, Director, Office of Science, Office of Basic Energy Sciences, Division of Materials Sciences and Engineering under Contract No. DESC0008505. L.R., A.A. and P.L. were funded by the Vannevar Bush Faculty Fellowship program sponsored by the Basic Research Office of the Assistant Secretary of Defense for Research and Engineering and funded by the Office of Naval Research through grant N00014-15-1-0045. X-ray diffraction was performed at the Stanford Nano Shared Facilities at Stanford University, supported by the National Science Foundation under Award No. ECCS-1542152.

[1] Ü. Özgür, Y. Alivov, and H. Morkoç, "Microwave ferrites, part 1: Fundamental properties," (2009).
[2] V. G. Harris, IEEE Trans. Magn. **48**, 1075 (2012).
[3] V. G. Harris, A. Geiler, Y. Chen, S. D. Yoon, M. Wu, A. Yang, Z. Chen, P. He, P. V. Parimi, X. Zuo, C. E. Patton, M. Abe, O. Acher, and C. Vittoria, J. Magn. Magn. Mater. **321**, 2035 (2009).
[4] P. D. Baba and G. M. Argentina, IEEE Trans. Microw. Theory Tech. **22**, 652 (1974).
[5] A. V. Chumak, V. Vasyuchka, A. Serga, and B. Hillebrands, Nat. Phys. **11**, 453 (2015).
[6] M. Farle, Reports Prog. Phys. **61**, 755 (1998).
[7] M. C. Onbasli, A. Kehlberger, D. H. Kim, G. Jakob, M. Kläui, A. V. Chumak, B. Hillebrands, and C. A. Ross, APL Mater. **2**, 106102 (2014).
[8] C. Safranski, I. Barsukov, H. K. Lee, T. Schneider, A. A. Jara, A. Smith, H. Chang, K. Lenz, J. Lindner, Y. Tserkovnyak, M. Wu, and I. N. Krivorotov, Nat. Commun. **8**, 117 (2017).
[9] J. Lustikova, Y. Shiomi, Z. Qiu, T. Kikkawa, R. Iguchi, K. Uchida, and E. Saitoh, Journal of Applied Physics **116**, 153902 (2014), https://doi.org/10.1063/1.4898161.
[10] H. Zhou, X. Fan, L. Ma, L. Cui, C. Jia, S. Zhou, Y. S. Gui, C.-M. Hu, and D. Xue, Applied Physics Letters **108**, 192408 (2016), https://doi.org/10.1063/1.4949555.
[11] O. d'Allivy Kelly, A. Anane, R. Bernard, J. Ben Youssef, C. Hahn, A. H. Molpeceres, C. Carrétéro, E. Jacquet, C. Deranlot, P. Bortolotti, R. Lebourgeois, J.-C. Mage, G. de Loubens, O. Klein, V. Cros, and A. Fert, Applied Physics Letters **103**, 082408 (2013), https://doi.org/10.1063/1.4819157.
[12] H. L. Wang, C. H. Du, Y. Pu, R. Adur, P. C. Hammel, and F. Y. Yang, Phys. Rev. Lett. **112**, 197201 (2014).
[13] B. M. Howe, S. Emori, H. Jeon, T. M. Oxholm, J. G. Jones, K. Mahalingam, Y. Zhuang, N. X. Sun, and G. J. Brown, IEEE Magnetics Letters **6**, 1 (2015).
[14] C. T. Wang, X. F. Liang, Y. Zhang, X. Liang, Y. P. Zhu, J. Qin, Y. Gao, B. Peng, N. X. Sun, and L. Bi, Phys. Rev. B **96** (2017), 10.1103/PhysRevB.96.224403.
[15] C. Vittoria, P. Lubitz, P. Hansen, and W. Tolksdorf, J. Appl. Phys. **57**, 3699 (1985).
[16] F. J. Rachford, M. Levy, R. M. Osgood, A. Kumar, and H. Bakhru, J. Appl. Phys. **87**, 6253 (2000).
[17] B. Hu, Y. Chen, Z. Su, S. Bennett, L. Burns, G. Uddin, K. Ziemer, and V. G. Harris, IEEE Trans. Magn. **49**, 4234 (2013).
[18] S. Emori, B. A. Gray, H.-M. Jeon, J. Peoples, M. Schmitt, K. Mahalingam, M. Hill, M. E. McConney, M. T. Gray, U. S. Alaan, A. C. Bornstein, P. Shafer, A. T. N'Diaye, E. Arenholz, G. Haugstad, K.-Y. Meng, F. Yang, D. Li, S. Mahat, D. G. Cahill, P. Dhagat, A. Jander, N. X. Sun, Y. Suzuki, and B. M. Howe, Adv. Mater. **29**, 1701130 (2017).
[19] S. Emori, D. Yi, S. Crossley, J. J. Wisser, P. P. Balakrishnan, B. Khodadadi, P. Shafer, C. Klewe, A. T. N'Diaye, B. T. Urwin, K. Mahalingam, B. M. Howe, H. Y. Hwang, E. Arenholz, and Y. Suzuki, Nano Letters **18**, 4273 (2018).
[20] L. J. Riddiford, J. J. Wisser, S. Emori, P. Li, D. Roy, E. Cogulu, O. van 't Erve, Y. Deng, S. X. Wang, B. T. Jonker, A. D. Kent, and Y. Suzuki, Appl. Phys. Lett. **115**, 122401 (2019).
[21] J. J. Wisser, S. Emori, L. Riddiford, A. Altman, P. Li, K. Mahalingam, B. T. Urwin, B. M. Howe, M. R. Page, A. J. Grutter, B. J. Kirby, and Y. Suzuki, Appl. Phys. Lett. **115**, 132404 (2019).
[22] J. Wisser, A. Grutter, D. Gilbert, A. N'diaye, C. Klewe, P. Shafer, E. Arenholz, Y. Suzuki, and S. Emori, In preparation (2019).
[23] M. Gray, S. Emori, B. Gray, H. Jeon, O. van 't Erve, B. Jonker, S. Kim, M. Suzuki, T. Ono, B. Howe, and Y. Suzuki, Phys. Rev. Appl. **9**, 064039 (2018).
[24] Y. Suzuki, Annual Review of Materials Research **31**, 265 (2001), https://doi.org/10.1146/annurev.matsci.31.1.265.
[25] A. V. Singh, B. Khodadadi, J. B. Mohammadi, S. Keshavarz, T. Mewes, D. S. Negi, R. Datta, Z. Galazka, R. Uecker, and A. Gupta, Advanced Materials **29**, 1701222 (2017).
[26] S. Brice-Profeta, M.-A. Arrio, E. Tronc, N. Menguy, I. Letard, C. C. dit Moulin, M. Nogues, C. Chanéac, J.-P. Jolivet, and P. Sainctavit, Journal of Magnetism and Magnetic Materials **288**, 354 (2005).
[27] J.-Y. Kim, T. Koo, and J.-H. Park, Physical review letters **96**, 047205 (2006).
[28] G. van der Laan and B. T. Thole, Phys. Rev. B **43**, 13401 (1991).